The Journal of Immunology

IL-21 Contributes to Fatal Inflammatory Disease in the Absence of Foxp3 $^{+}$ T Regulatory Cells

Alexis Vogelzang, Helen M. McGuire, Sue M. Liu, Brian Gloss, Karessa Mercado, Peter Earls, Marcel E. Dinger, Marcel Batten, Jonathan Sprent and Cecile King

J Immunol 2014; 192:1404-1414; Prepublished online 20 January 2014;
doi: 10.4049/jimmunol.1302285
http://www.jimmunol.org/content/192/4/1404

The Journal of Immunology is published twice each month by
The American Association of Immunologists, Inc.,
9650 Rockville Pike, Bethesda, MD 20814-3994.

Print ISSN: 0022-1767 Online ISSN: 1550-6606.

IL-21 Contributes to Fatal Inflammatory Disease in the Absence of Foxp3$^+$ T Regulatory Cells

Alexis Vogelzang,[*,†] Helen M. McGuire,[*,†] Sue M. Liu,[*,†] Brian Gloss,[‡] Karessa Mercado,[*,†] Peter Earls,[§] Marcel E. Dinger,[‡] Marcel Batten,[*,†] Jonathan Sprent,[*,†,¶] and Cecile King[*,†]

The cytokine IL-21 has been shown to influence immune responses through both costimulatory effects on effector T cells and opposing inhibitory effects on T regulatory cells (Tregs). To distinguish the effect of IL-21 on the immune system from that of its effect on Tregs, we analyzed the role of IL-21/IL-21R signaling in mice made genetically deficient in IL-2, which exhibit a deficit in IL-2–dependent Foxp3 regulatory T cells and suffer from a fatal multiorgan inflammatory disease. Our findings demonstrate that in the absence of IL-21/IL-21R signaling, *Il2*$^{-/-}$ mice retained a deficiency in Tregs yet exhibited a reduced and delayed inflammatory disease. The improved health of *Il2*$^{-/-}$*Il21r*$^{-/-}$ mice was reflected in reduced pancreatitis and hemolytic anemia and this was associated with distinct changes in lymphocyte effector populations, including the reduced expansion of both T follicular helper cells and Th17 cells and a compensatory increase in IL-22 in the absence of IL-21R. IL-21/IL-21R interactions were also important for the expansion of effector and memory CD8$^+$ T cells, which were critical for the development of pancreatitis in *Il2*$^{-/-}$ mice. These findings demonstrate that IL-21 is a major target of immune system regulation. ***The Journal of Immunology*****, 2014, 192: 1404–1414.**

The two γ-chain family cytokines IL-2 and IL-21 lie adjacent to each other on chromosome 3 in mice and on chromosome 4 in humans. Both cytokines are produced by CD4$^+$ T cells following TCR ligation, yet IL-2 and IL-21 are autocrine growth factors for distinct T helper subsets with regulatory and effector functions, respectively. IL-2 is a survival factor for peripheral Foxp3-expressing T regulatory cells (Tregs), which are vital for regulating immune responses and tolerance to self-tissues (1). Conversely, IL-21 plays an important role in the survival/differentiation of several CD4$^+$ T effector subsets (2) and supports the long-term survival of CD8$^+$ T cells during chronic viral infections (3, 4). Additionally, IL-21 has been reported to have an inhibitory effect on Tregs (5). Consistent with these actions on lymphocyte populations, IL-21 contributes to the development of inflammatory and autoimmune diseases in several animal models such as colitis, systemic lupus erythematosus, experimental autoimmune encephalomyelitis, type 1 diabetes, and rheumatoid arthritis (2). However, the mechanisms explaining the function of IL-21 in autoimmune disease pathogenesis remain unknown.

Our current understanding of inflammatory diseases affecting organs of the digestive system proposes a combination of genetic predisposition and environmental interactions with the mucosa and immune system. Mice made genetically deficient in IL-2 or its high-affinity receptor chain (CD25) suffer from a fatal inflammatory disease characterized by ulcerative colitis and hemolytic anemia (6). This fatal multiorgan inflammatory disease is caused by a failure to regulate effector T cells due to a deficit of IL-2–dependent Foxp3 Tregs (1, 6, 7). The observation that germ-free *Il2*$^{-/-}$ mice have delayed and milder intestinal infiltration indicates that multiorgan inflammatory disease results from a defect in peripheral tolerance mechanisms toward mucosal commensal Ags (8, 9). The caveat inherent in the study of gastrointestinal disorders in germ-free mice is that commensal micro-organisms are required for the normal development of the gastrointestinal mucosal immune system (10). However, analyses of germ-free *Il2*$^{-/-}$ mice with monocultures of specific commensals support the notion that gut microbes modulate colitis (11, 12). Previous studies have shown that mice genetically deficient in both CD25 and CD4$^+$ T cells lack the severe colitis present in *Cd25*$^{-/-}$ mice and that treatment of *Il2*$^{-/-}$ mice with anti-CD40L mAbs prevented disease (6, 13). Thus, CD4$^+$ T cells are responsible for the destructive immune infiltration in mucosal tissues in *Il2*$^{-/-}$ mice. However, the mechanisms underlying CD4$^+$ T cell–mediated disease in *Il2*$^{-/-}$ mice remain unknown.

Previous studies have demonstrated that IL-2–dependent Tregs are necessary for the maintenance of immune tolerance to self-tissues. In this study we provide evidence that the CD4$^+$ T helper cytokine IL-21 plays an important role in the fatal inflammatory disease in *Il2*$^{-/-}$ mice and is thus a central target of immune regulation.

[*]Department of Immunology, Garvan Institute of Medical Research, Darlinghurst, New South Wales 2010, Australia; [†]St. Vincent's Clinical School, University of New South Wales, Sydney, New South Wales 2010, Australia; [‡]Clinical Genomics Kinghorn Cancer Centre, Darlinghurst, New South Wales 2010, Australia; [§]Department of Anatomical Pathology, St. Vincent's Hospital, Darlinghurst, New South Wales 2010, Australia; and [¶]World Class University Program, Division of Integrative Biosciences and Biotechnology, Pohang University of Science and Technology, Pohang 790-784, Korea

Received for publication August 28, 2013. Accepted for publication December 4, 2013.

This work was supported by grants from the National Health and Medical Research Council and the Rebecca L. Cooper Foundation.

A.V. performed experiments, analyzed data, and wrote the manuscript; H.M., S.M.L., K.M., and B.G. performed experiments; P.E., M.D., and B.G. analyzed data; J.S. provided reagents; and C.K. designed the research, analyzed data, and wrote the manuscript.

Address correspondence and reprint requests to Dr. Cecile King, Garvan Institute of Medical Research, 384 Victoria Street, Darlinghurst, NSW 2010, Australia. E-mail address: c.king@garvan.org.au

The online version of this article contains supplemental material.

Abbreviations used in this article: GC, germinal center; IEL, intraepithelial lymphocyte; LPL, lamina propria lymphocyte; MLN, mesenteric lymph node; MZ, marginal zone; Tfh, T follicular helper; Treg, T regulatory cell; WT, wild-type.

www.jimmunol.org/cgi/doi/10.4049/jimmunol.1302285

Materials and Methods

Mice

Il21r$^{-/-}$ mice (Dr. Warren Leonard, National Institutes of Health) at C57BL/6 N6 and backcrossed to N10 for experimental use; the resulting mice were >99.8% C57BL/6 as determined by a genome scan of 600+ markers. C57BL/6 (N10) *Il2*$^{+/-}$ mice, purchased from The Jackson Laboratory (Bar Harbor, ME), were crossed onto *Il21r*$^{+/-}$ in-house to create wild-type (WT), *Il21r*$^{-/-}$, *Il2*$^{-/-}$, and *Il21r*$^{-/-}$*Il2*$^{-/-}$ mice. PCR was performed to determine whether the *Il2*$^{-/-}$ mice carried the IL-21 allele from 129 mice, as described previously (14). Animals were housed under specific pathogen-free conditions and handled in accordance with the Australian Code of Practice for the Care and Use of Animals for Scientific Purposes.

RNA was isolated from splenocytes using using TRIzol reagent (Invitrogen) and quantitation of IL-21 mRNA was performed on a 2100 Bioanalyzer (Agilent Technologies, Santa Clara, CA) as described previously (14).

RNA sequencing

RNA from MACS-purified CD4$^+$ T cells was extracted and DNAse treated using the RNeasy kit (Qiagen) according to the manufacturer's instructions. RNA integrity was assessed as >9 on the Bioanalyzer RNA nanochip (Agilent Technologies). Strand-specific RNA sequencing libraries of poly(A) RNA from 500 ng total RNA were generated using the SureSelect strand-specific RNA library prep for Illumina multiplexed sequencing (Agilent Technologies). Libraries were sequenced (100 bp, paired-end) on the Illumina 2500 platform at the Centre for Clinical Genomics (Garvan Insititue) and FASTQ files were analyzed.

Sequencing data (20,256,959 reads for WT and 33,582,698 for knockout) were checked for sequencing quality by FastQC (http://www.bioinformatics.babraham.ac.uk/projects/fastqc/) and species purity by FastQ Screen (http://www.bioinformatics.babraham.ac.uk/projects/fastq_screen/). Next adaptor and poor quality sequences were removed using Trim Galore (~5% reads removed) (http://www.bioinformatics.babraham.ac.uk/projects/trim_galore/). Mapping and differential gene expression was performed as previously shown (15). Briefly, sequences were mapped to mm10 by Tophat2 (16) using Ensembl (GRC38) gene annotations; 90% of sequences were mapped. Gene level count data were assessed using HTSeq count (http://www-huber.embl.de/users/anders/HTSeq/doc/overview.html) against Ensembl genes (GRC38) and analyzed by DESeq (17) in the R statistical environment version 3.0 (http://www.r-project.org/). Count dispersion was estimated from global counts data for single replicates as indicated in the DESeq manual. Significant differential expression was established by an adjusted p value of <0.05.

Flow cytometry

Abs purchased from BD Biosciences were $\alpha_4\beta_7$-PE, B220-PerCP-Cy5.5, CD11b-PE, CD11c-allophycocyanin, CXCR5-biotin, GL7-FITC, granzyme B–PE, IL-10–allophycocyanin, Syndecam-1–PE. Abs purchased from eBioscience were CD3–Pacific Blue, CD4–Alexa Fluor 750, CD8-PerCP-Cy5.5, CD19–Pacific Blue, CD44-allophycocyanin, Foxp3–Alexa Fluor 647, ICOS-PE, IL-17A–FITC, INF-α–FITC, TNF-α–PE, and IL-22–PE (BioLegend). IL-21R-Fc chimera (R&D Systems) was used to detect IL-21. Cells were acquired using a FACSCanto II cytometer (BD Biosciences, San Diego, CA) and analyzed using FlowJo (Tree Star, Ashland, OR). Intracellular cytokines were detected either directly ex vivo or after 4 h stimulation at 37°C (5 ng/ml PMA, 1 μg/ml ionomycin, and GolgiStop; 1:1000; BD Biosciences) using the BD Biosciences intracellular staining kit according to the manufacturer's instructions.

Treg suppression assay

CD4$^+$CD25$^+$ Tregs or CD4$^+$CD25$^-$ T responder populations were sorted from lymphocyte preparations to high purity using a FACSAria. T responders were labeled with 0.05 M CFSE. Plate-bound APCs were obtained by incubation of RBC-depleted splenocytes on 15-cm cell culture plates at 37°C for 2 h. ^{137}Cs source (2 Gy) irradiated APCs (8×10^4) with 0.5 μg/ml soluble anti-CD3 (145.2C11) were cultured with 1×10^5 T responders and a 1:1 to 1:16 ratio of T responders to Tregs. Cells were analyzed after 72 h by flow cytometry, and the proportion of divided CFSE$^+$CD4$^+$ T responders was calculated by gating on diluted CFSE peaks.

Histology

Five-micrometer frozen Tissue-Tek OCT tissue sections were fixed in ice-cold acetone. Primary biotin-, FITC-, or Alexa Fluor 647–conjugated Abs were incubated in 100 μl at room temperature for 2 h followed by amplification with streptavidin-Cy3 (Jackson ImmunoResearch Laboratories) for 1 h. Tissues in 10% formalin were embedded in paraffin and 4-μm sections were stained with H&E by the Garvan Institute histology facility. Sections were analyzed using a Leica DM RBE TCS confocal microscope or Leica light microscope (Leica Microsystems, Wetzlar, Germany). The images were processed using the Leica acquisition and analysis software and Adobe Photoshop, version 7 (Adobe Systems, San Jose, CA).

ELISA and cytokine detection

Serum Ig was captured using anti-mouse Ig(H+L) (2 μg/ml; SouthernBiotech). Analytes were detected using alkaline phosphatase–conjugated anti-mouse IgG, IgG1, IgG2b, IgG2c, IgM, and IgA (1:2000 SouthernBiotech) compared with standards for each isotype (1 μg/ml; SouthernBiotech). IgE was analyzed using the BD Biosciences kit according to the manufacturer's instructions. Cytokine bead array analysis of serum was carried out using a FlowCytomix mouse Th1/Th2 multiplex including an IL-22 simplex assay from Bender MedSystems. IL-21 was detected with IL-21R Fc chimera (R&D Systems) followed by an anti-human IgG1 secondary Ab using the BD Biosciences intracellular immunostaining kit according to the manufacturer's instructions. RNA was isolated from splenocytes following stimulation with anti-CD3 and anti-CD28 mAbs using using TRIzol reagent (Invitrogen) and quantitation of IL-21 mRNA performed on a 2100 Bioanalyzer as described previously (14).

Intracolonic lymphocyte isolation

Peyer's patches were removed and the colon was cut longitudinally and cleaned. Tissues were incubated in 20 ml intraepithelial lymphocyte (IEL) stripping buffer (1 mM EDTA, 1 mM DTT, 5% FCS, 50 μg/ml penicillin-streptomycin in PBS) for 20 min at 37°C while shaking. Lymphocytes in the supernatant were isolated by Percoll (GE Healthcare) gradient. To isolate the lamina propria lymphocytes (LPLs), the tissue remaining after treatment with stripping buffer was digested in 15 ml 5 mg/ml collagenase D (Roche) and 0.05% DNAse (Promega) in lymphocyte isolation media. These cells were run on a Percoll gradient and analyzed.

Pancreatitis scoring

Routine H&E staining for determination of organ inflammation was performed on 4-μm paraffin-embedded sections using standard procedures. Histopathological evaluation of pancreatic lesions was performed by light microscopy. The severity of inflammation was determined by blinded scoring of the degree of inflammatory cell infiltration into tissues as described by Kanno et al. (18) (0, none; 1, mild; 2, moderate; 3, moderate and diffuse or severe but focal; 4, severe and diffuse).

Statistical analysis

Data were analyzed using Prism software (Graphpad Software, San Diego, CA) to calculate an unpaired, two-way Student t test, with an F test to compare variances. Analysis of more that two groups was performed using one-way ANOVA followed by Bonferroni's posttest.

Results

Elevated IL-21 production in Il2$^{-/-}$ *mice*

The genes for IL-2 and IL-21 sit adjacent to each other on chromosome 3 in mice and on chromosome 4 in humans, and a wide body of literature from genome-wide association studies has identified the *Il2/Il21* locus as a susceptibility locus for chronic inflammatory and autoimmune diseases. *Il2*$^{-/-}$ mice were examined to determine whether IL-2 deficiency influenced IL-21 production. To obtain a broad, unbiased view of the transcriptome of CD4$^+$ T cells from *Il2*$^{-/-}$ mice, we performed RNA sequencing on unstimulated CD4$^+$ T cells purified from the spleens of both *Il2*$^{-/-}$ and WT mice. CD4$^+$ T cells from *Il2*$^{-/-}$ mice demonstrated increased levels of IL-21 mRNA relative to WT CD4$^+$ T cells (Fig. 1A). Differential gene expression analyses revealed that *Il21* was one of the top 10 most highly expressed genes in *Il2*$^{-/-}$ CD4$^+$ T cells, relative to WT CD4$^+$ T cells (Fig. 1B). The fact that

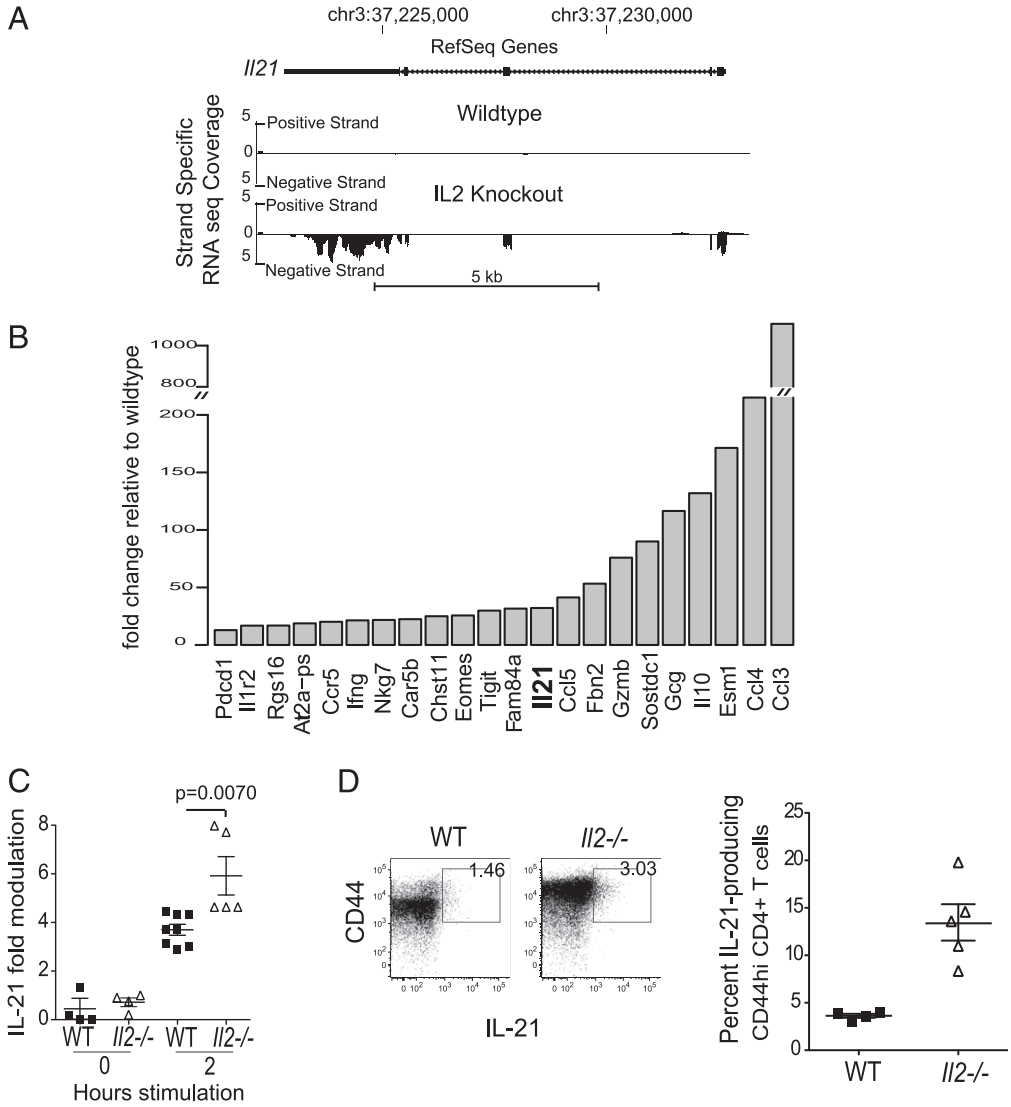

FIGURE 1. Increased production of IL-21 in $Il2^{-/-}$ mice. (**A**) Strand-specific RNAseq read coverage of IL-21 locus in WT and IL-2 knockout cells. Read depth mapped to each strand at the IL-2 locus was visualized in the University of California, Santa Cruz genome browser (http://www.ncbi.nlm.nih.gov/bioproject/231953). The IL-21 gene, transcribed from the negative strand (RefSeqGene), has greater coverage in knockout cells (32-fold; adjusted p of <0.003). (**B**) Fold change of gene expression in IL-2 knockout T cells relative to WT for significantly upregulated genes (adjusted p of <0.05). Fold change was calculated from normalized HTseq counts data for each gene. (**C**) IL-21 mRNA levels from WT and $Il2^{-/-}$ splenocytes ex vivo (T0) and after 2 h stimulation with soluble anti-CD3 and anti-CD28 mAbs measured by real-time PCR. IL-21 mRNA expression is presented as fold modulation compared with WT ex vivo levels; data are representative of two experiments where $n = 3$–8 mice. (**D**) Percentage IL-21–producing $CD44^{hi}CD4^+$ T cells in the spleen of $Il2^{-/-}$ mice and B6 littermates, determined by intracellular immunostaining and FACS. Representative histograms showing intracellular IL-21 staining of $CD4^+$ T cells compared with $Il21^{-/-}$ $CD4^+$ T cells as a control. Data are representative of two experiments where $n = 3$.

strong transcription of *Il21* was observed in $Il2^{-/-}$ mice is made all the more notable by the fact that the source of RNA was unstimulated $CD4^+$ T cells. Confirmed by quantitative PCR, IL-21 mRNA levels were greater in $Il2^{-/-}$ $CD4^+$ T cells 2 h after stimulation with mAbs against CD3 and CD28 in vitro (Fig. 1C). This finding correlated with an increased fraction of IL-21–producing $CD4^+$ T cells relative to WT $CD4^+$ T cells ex vivo (Fig. 1D).

Sustained Treg defect in the absence of IL-21

To investigate the possible role of IL-21 in the inflammatory disease of $Il2^{-/-}$ mice, we crossed $Il2^{-/+}$ mice with $Il21r^{-/+}$ mice to generate $Il2^{-/-}Il21r^{-/-}$ double knockout mice and $Il2^{-/-}$, $Il21r^{-/-}$, and WT littermates. As noted previously, $Il2^{-/-}$ mice have a deficiency of $CD25^+Foxp3^+CD4^+$ Tregs, and $Il2^{-/-}Il21r^{-/-}$ mice similarly exhibited a deficit of Tregs in the spleen (Fig. 2A, 2B), mesenteric lymph nodes (MLNs) (Fig. 2C), and lamina propria of the colon (LPLs) (Fig. 2D). However, there was a trend of increased absolute numbers of $Foxp3^+$ cells in $Il2^{-/-}$ and $Il2^{-/-}Il21r^{-/-}$ tissues relative to WT and $Il21r^{-/-}$ tissues due to the large expansion of the $CD4^+$ T cell subset in the former two groups (Supplemental Fig. 1). IL-21 did not inhibit the function of Tregs in vitro, which were equally capable of suppressing the proliferation of both WT and $Il21r^{-/-}$ $CD25^-CD4^+$ effector cells (Supplemental Fig. 1).

In accordance with the observed Treg deficiency, the splenomegaly observed in $Il2^{-/-}$ littermates was not influenced by the absence of IL-21/IL-21R signaling (Fig. 2E). Quantification of cells in the spleen (Fig. 2F), MLN (Fig. 2G), and lamina propria of the colon (Fig. 2H), which is a site of inflammation in $Il2^{-/-}$ mice, showed increased numbers in both $Il2^{-/-}Il21r^{-/-}$ and $Il2^{-/-}$ mice relative to WT and $Il21r^{-/-}$ littermates.

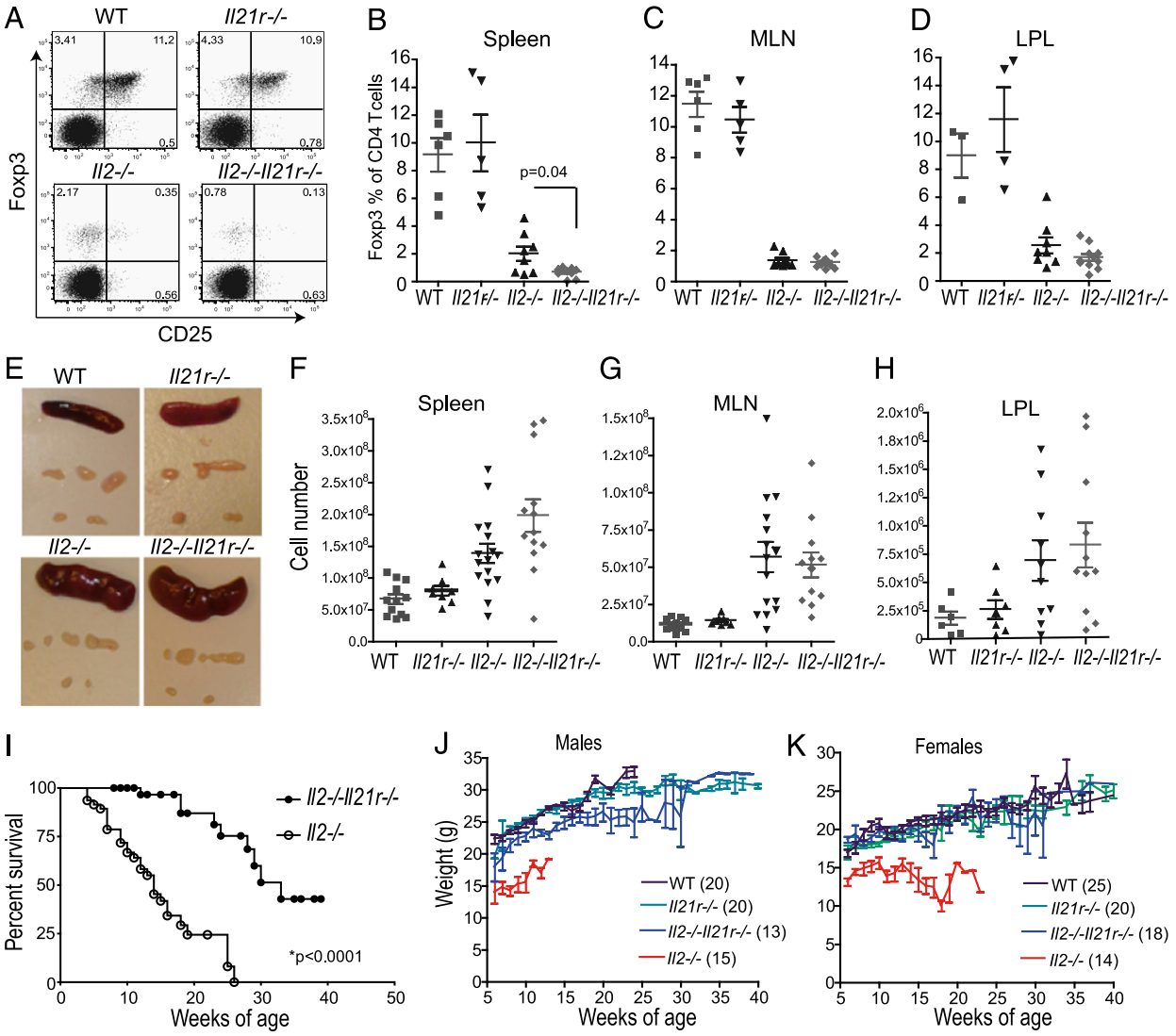

FIGURE 2. IL-21R deficiency reduces mortality in $Il2^{-/-}$ mice. (**A**) Representative flow cytometry dot plots from MLNs showing $Foxp3^{+}CD25^{+}$ Tregs gated on $CD4^{+}CD3^{+}$ T cells. Quantification of $Foxp3^{+}$ cells from (**B**) spleen, (**C**) MLNs, and (**D**) LPLs as a proportion of $CD4^{+}CD3^{+}$ T cells shown as individual mice and means ± SEM. Data are from three experiments with 5–10 mice per group. (**E**) Representative images of spleens, MLNs, and inguinal lymph nodes from WT, $Il21r^{-/-}$, $Il2^{-/-}$, and $Il2^{-/-}Il21r^{-/-}$ mice. Absolute cell numbers from the (**F**) spleen, (**G**) MLNs, and lymphocyte isolations of the (**H**) LPLs. Data show values from 8–15 individual mice plus the means ± SEM from five experiments. Genotypes were compared using one-way ANOVA and a Bonferroni posttest to compare $Il2^{-/-}$ and $Il2^{-/-}Il21r^{-/-}$ values. (**I**) Percentage survival of $Il2^{-/-}Il21r^{-/-}$ ($n = 31$) and $Il2^{-/-}$ mice ($n = 29$) was measured using euthanasia as an endpoint when mice lost 20% of their weight, or when severe morbidity was observed. A χ^2 log-rank test was used to compare survival curves. Cumulative weights of (**J**) male and (**K**) female WT, $Il21r^{-/-}$, and $Il2^{-/-}$ mice and $Il2^{-/-}Il21r^{-/-}$ littermate data show the means ± SEM.

IL-21 drives inflammatory disease in the absence of Fox-P3 Tregs

As mentioned earlier, the chronic inflammatory disease observed in $Il2^{-/-}$ mice has been attributed to the deficiency of IL-2–dependent Tregs (1, 6). However, it was immediately evident from the healthy appearance of $Il2^{-/-}Il21r^{-/-}$ mice that despite an equally profound reduction in the percentage of Tregs, removing IL-21/IL-21R signaling had mitigated disease. Both morbidity and mortality were significantly delayed and reduced in $Il2^{-/-}Il21r^{-/-}$ mice (Fig. 2I). The improved health of $Il2^{-/-}Il21r^{-/-}$ mice was evident in the weights of both sexes that were equivalent to WT and $Il21r^{-/-}$ mice and significantly increased compared with $Il2^{-/-}$ littermates ($p < 0.0001$) (Fig. 2J, 2K). When the weights of individual mice were compiled, the weights of $Il2^{-/-}$ mice reflected early wasting disease with an almost universal downward trend, which was observed in only 15% of $Il2^{-/-}Il21r^{-/-}$ mice after 24 wk of age (data not shown).

Diminished target organ damage in the absence of IL-21/IL-21R signaling

Histological analyses were carried out on several organs to determine whether the improved morbidity and mortality in the absence of IL-21 corresponded with reduced tissue damage. The colon has been previously described as the target of the most severe cellular infiltrate in $Il2^{-/-}$ mice (6), and we observed frequent gut-associated lymphoid structures that were enlarged in both $Il2^{-/-}$ and $Il2^{-/-}Il21r^{-/-}$ strains (Fig. 3A). There was evidence of increased mononuclear lymphocytes found throughout both the mucosa and lamina propria (Fig. 3A–C). Despite registering these frequent signs of inflammation, we observed little ulceration, crypt abscesses, or erosive destruction of the mucosa in the samples

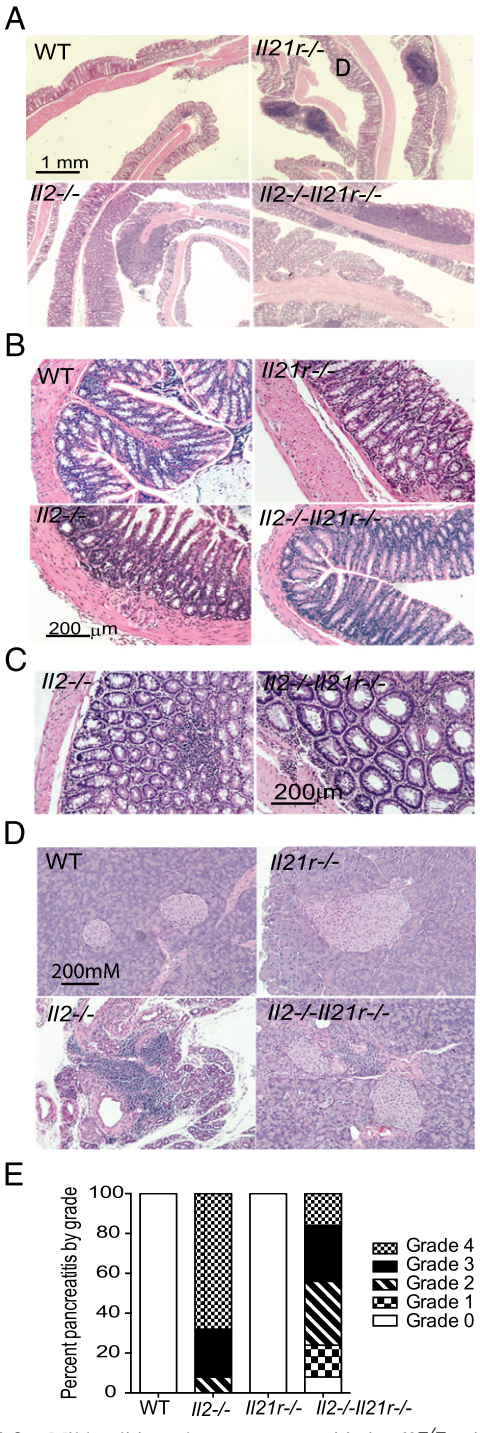

FIGURE 3. Mild colitis and severe pancreatitis in $Il2^{-/-}$ mice is improved in the absence of IL-21R. (**A**) Representative H&E-stained histological sections of the distal colon from indicated genotypes showing (**B**) crypt branching and (**C**) mononuclear cell infiltrate in $Il2^{-/-}$ strains. (**D**) Representative H&E-stained histological sections of pancreata from indicated genotypes. (**E**) Pancreatitis grade from histological sections of indicated genotypes. At least 10 sections were assessed throughout the pancreas per mouse. Colon and pancreata samples were obtained from 10- to 14-wk-old mice; $n = 10$ for WT and $Il21r^{-/-}$ samples and $n = 10$–15 for $Il2^{-/-}$ and $Il2^{-/-}Il21r^{-/-}$ strains.

studied and large areas retained structural, apparently functional integrity (Fig. 3A–C).

This assessment led us to examine other tissues for damage that may have been able to explain the wasting disease observed in $Il2^{-/-}$ mice. The severe weight loss in $Il2^{-/-}$ mice made the pancreas a candidate organ for pathology. Pancreatic islets remained undamaged by infiltrate in both strains (Fig. 3D). In contrast, we found that in our colony and specific pathogen-free housing conditions, 90% of pancreatic samples from both strains at the age of 9–12 wk contained diffuse lymphocytic aggregates that were both parenchymal and perivascular (Fig. 3D). However, it was clear that in the absence of IL-21/IL-21R signaling, the observed inflammation was reduced and there was an associated improvement in the level of parenchymal damage inflicted with minimal to sporadic damage of exocrine tissue, whereas atrophied serous acini and loss of the lobular architecture was widespread in all $Il2^{-/-}$ pancreata (Fig. 3D). These changes were consistent and reflected by the reduced grade of inflammation and exocrine damage in the absence of IL-21/IL-21R signaling (Fig. 3E).

IL-21 promotes the production of class-switched Ab in $Il2^{-/-}$ mice

In the $Il2^{-/-}$ model, B cells are initially stimulated to make large amounts of class-switched Ab, which is thought to target self-Ags (6). This harmful B cell activation is ameliorated in surviving older mice as the B cell population undergoes a rapid decline (19). B cells showed a mild increase as both a percentage of lymphocytes and absolute numbers in the spleen (Fig. 4A) and as a percentage of lymphocytes in the MLNs (Fig. 4B) and in the lamina propria (Fig. 4C) of $Il2^{-/-}Il21r^{-/-}$ mice relative to $Il2^{-/-}$ mice between 9 and 12 wk of age. However, the most striking observation was that the lymphoid organs of both $Il2^{-/-}$ and $Il2^{-/-}Il21r^{-/-}$ mice had significantly less B cells compared with WT and $Il21r^{-/-}$ littermates (Fig. 4A–C).

The phenotype of the B cells within this time frame was different, because both strains of $Il2^{-/-}$ mice contained germinal center (GC) and plasma phenotype B cells, despite the depleted total B cell population in these mice. However, IL-21/IL-21R signaling significantly increased the fractions, but not absolute numbers, of GC B cells (Fig. 4D, Supplemental Fig. 2) and the percentage of plasma B cells (Fig. 4E). The populations of marginal zone (MZ) B cells were compromised in both $Il2^{-/-}$ and $Il2^{-/-}Il21r^{-/-}$ mice relative to WT and $Il21r^{-/-}$ littermates (Fig. 4F). Taken together, these findings demonstrate the importance of IL-21/IL-21R signaling for GC B cells and plasma cells during autoimmunity.

T follicular helper (Tfh) cells provide cognate help to B cells for the production of class-switched, affinity-matured Abs during GC reactions, and previous work from our laboratory and others indicated that IL-21 was an important survival/differentiation factor for $CXCR5^{hi}ICOS^{hi}$ Tfh cells and $CXCR5^{hi}PD\text{-}1^{hi}$ Tfh cells (20–22). In agreement with this observation, $CXCR5^{hi}$ and $ICOS^{hi}$ Tfh cells (Supplemental Fig. 2) were elevated in $Il2^{-/-}$ mice in an IL-21–dependent manner.

Measurement of serum Ab levels using ELISA suggested that Ab production in $Il2^{-/-}$ mice was dependent on IL-21. Indeed, despite the inflammation observed in $Il2^{-/-}Il21r^{-/-}$ mice, the T-dependent Ig isotypes IgG1 and IgG2c were comparable to resting WT levels rather than the high circulating Ab levels observed in the $Il2^{-/-}$ sera (Fig. 5A). This was evident in $Il2^{-/-}$ mice under 11 wk of age when significant numbers of B cells remained, and also from the few long-lived Ab-secreting cells that had survived at the later time points studied (Fig. 5A).

IgA is typically produced at mucosal sites due to its stable dimer formation that allows transport into the gastrointestinal tract and resistance to high pH, and it can be produced in response to both T-dependent and -independent Ags (23). IL-21 influenced IgA production, as levels were significantly reduced in $Il2^{-/-}Il21r^{-/-}$

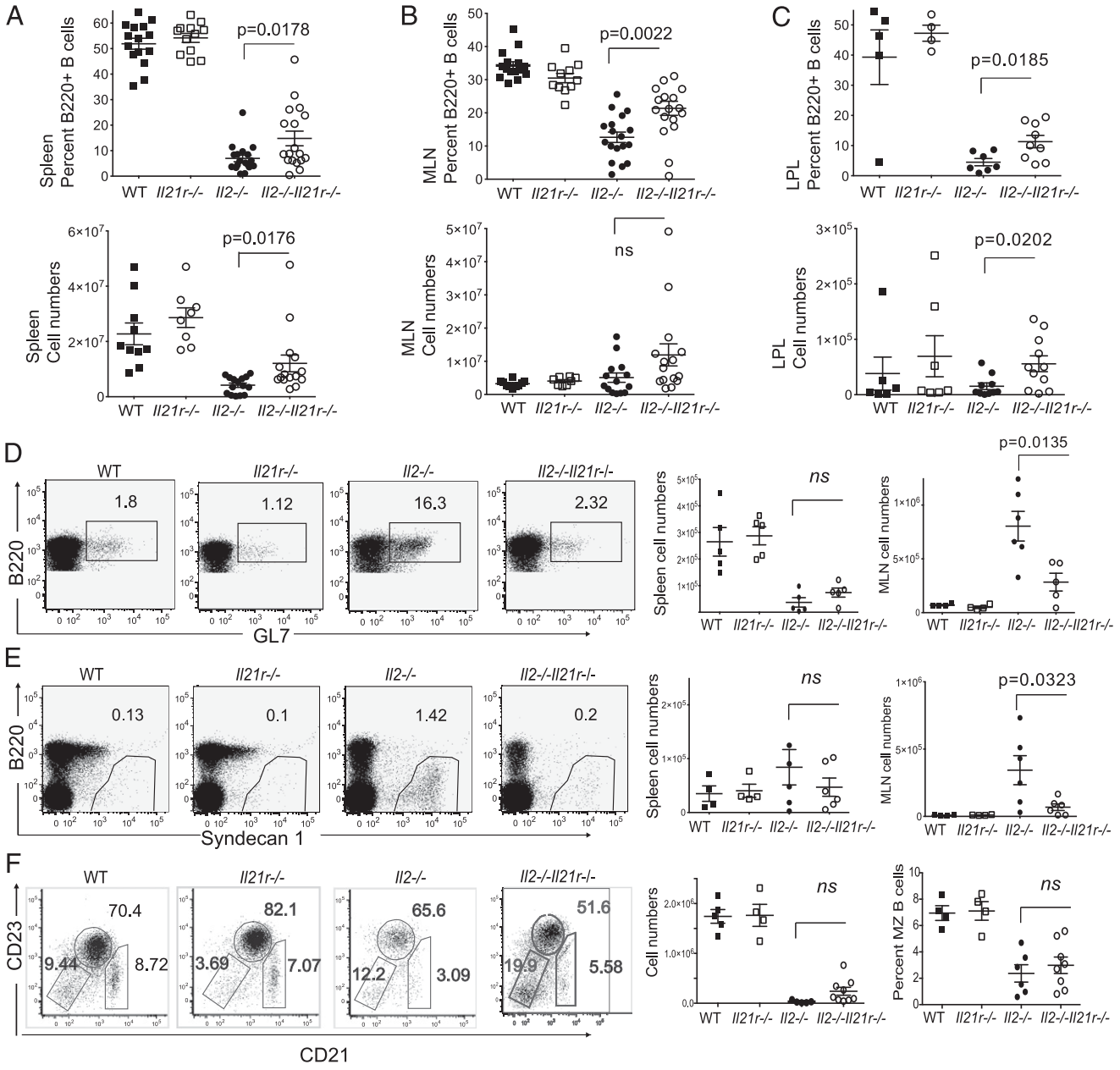

FIGURE 4. B cell differentiation in *Il2*$^{-/-}$ mice is influenced by IL-21. Percentages and total numbers of CD19^{+} B cells in (**A**) the spleen, (**B**) MLNs, and (**C**) LPLs of the large intestine of 11-wk-old WT, *Il21r*$^{-/-}$, *Il2*$^{-/-}$, and *Il2*$^{-/-}$*Il21r*$^{-/-}$ mice; n = 7–15 mice per group from four experiments. Flow cytometric analyses from the MLNs of these mice showing representative dot plots and quantitation of (**D**) percentage GL7^{+} GC CD19^{+} B cells, (**E**) percentage and absolute numbers of Syndecan-1^{+}CD19^{+} plasma cells, and (**F**) percentage and absolute numbers of CD19^{+}CD23^{lo}CD21^{hi} MZ B cells.

sera relative to *Il2*$^{-/-}$ sera (Fig. 5A). IgM was likely affected by the reduced B cell numbers in both *Il2*$^{-/-}$ strains that exhibited low levels both in the presence and absence of IL-21 (Fig. 5A). IgE was similarly unaffected by IL-21 and was elevated in both *Il2*$^{-/-}$ strains, despite the previously described increase observed in single *Il21r*$^{-/-}$ mice (Supplemental Fig. 2). The finding that the IgE isotype was not affected by the increase in Tfh cells and GC B cells in *Il2*$^{-/-}$ mice agrees with reports that IgE class switch and production can result from both T-dependent extrafollicular as well as T-independent pathways (24).

Hemolytic anemia is reduced in the absence of IL-21/IL-21R signaling

The hemolytic anemia observed in 80% of *Il2*$^{-/-}$ mice (6) is absent in *JH*$^{-/-}$*Il2*$^{-/-}$ double knockout mice, indicating that B cells are critical for hemolytic anemia in *Il2*$^{-/-}$ mice (25) but present in germ-free *Il2*$^{-/-}$ mice and may therefore reflect self-reactivity in the absence of regulation (8). In accordance with the reduced Ab produced in the absence of IL-21/IL-21R signaling, hemolytic anemia was less severe in *Il2*$^{-/-}$*Il21r*$^{-/-}$ mice as shown by a higher hematocrit (packed RBC volume as a percentage of total serum) (Fig. 5B).

IL-21 shapes the serum cytokine profile during chronic inflammation

To determine how IL-21 shaped the global serum cytokine profile in *Il2*$^{-/-}$ mice, we measured levels of a variety of inflammatory cytokines using a flow cytometry cytokine bead array method that compared relative mean fluorescence intensity in serum samples. Consistent with the improved lifespan of the double knockout mice, the loss of IL-21/IL-21R signaling led to an increased frequency of mice with the immunosuppressive cytokines IL-4 and

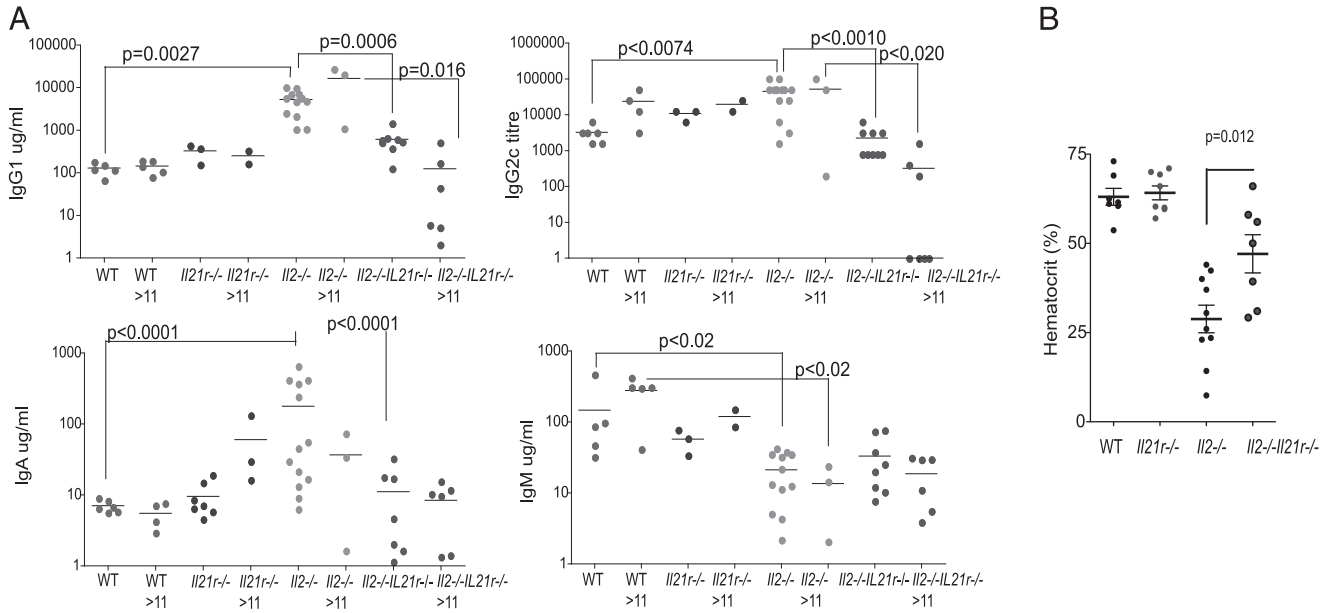

FIGURE 5. Ab production and hemolytic anemia in *Il2*$^{-/-}$ mice is dependent on IL-21. (**A**) Quantification of the $\log_{10}$ of serum Ab isotype concentrations or titer measured by ELISA in young (<11 wk of age) and mature (>11 wk of age) mice. Data show the mean and individual values from mice from two separate experiments. The *p* values were calculated comparing similar age groups using a Student *t* test. (**B**) Hematocrit (percentage RBC volume of whole blood) values from individual mice between 6 and 10 wk of age as shown.

IL-10 in sera (Fig. 6A). Paradoxically, a greater number of *Il2*$^{-/-}$ *Il21r*$^{-/-}$ mice also harbored the proinflammatory cytokines TNF-α, IL-1a, and GM-CSF in sera (Fig. 6A). In contrast, IL-23 was equally detected in the sera of both *Il2*$^{-/-}$ strains (Fig. 6A).

IL-17–producing Th17 cells induce chronic intestinal inflammation (26), and IL-21 produced by Th17 cells has been shown to create a positive feedback loop that supports the expansion of this population (27, 28). In support of this finding, a greater number of *Il2*$^{-/-}$ mice (56%) had circulating IL-17A than did *Il2*$^{-/-}$*Il21r*$^{-/-}$ mice (19%) (Fig. 6A). It was of interest to observe that IL-22 was distinctly affected by IL-21R deficiency, being detected in 65% of *Il2*$^{-/-}$*Il21r*$^{-/-}$ sera and 29% of *Il21r*$^{-/-}$ sera, but it was not detected in either *Il2*$^{-/-}$ or WT sera (Fig. 6A), implying that IL-21 may limit IL-22 production or IL-22–producing cells or that there was reduced utilization of IL-22 in the absence of IL-21/IL-21R signaling.

Altered T cell effector phenotype in Il2$^{-/-}$ *mice in the absence of IL-21*

The importance of thymocytes in the inflammatory disorder of *Il2*$^{-/-}$ strains was previously established in experiments that used athymic *Il2*$^{-/-}$ mice to demonstrate that disease progression in this model is dependent on T cells (7). By introducing IL-21R deficiency to the *Il2*$^{-/-}$ strain, we had hoped to pinpoint roles for IL-21 in CD4$^+$ T cell effector phenotypes that mediated tissue damage in this model. However, we could identify few differences between the numbers of T cells with an activated or memory surface phenotype in *Il2*$^{-/-}$ mice in the presence or absence of IL-21. CD44^{hi}CD4$^+$ T cells dominated the T cell compartment and ~20% of activated/memory phenotype CD4$^+$ T cells expressed the mucosal homing marker $\alpha_4\beta_7$ (Fig. 6B), which drives homing of activated cells to the mucosal surfaces where tissue damage in *Il2*$^{-/-}$ mice occurs (6, 13, 29).

In accordance with the similar failure to regulate the size of the T cell compartments, *Il2*$^{-/-}$ and *Il2*$^{-/-}$*Il21r*$^{-/-}$ mice exhibited a similar expansion of IFN-γ–producing Th1 cells that, for *Il2*$^{-/-}$ mice, was consistent with the increased expression of IFN-γ detected by RNAseq analyses of *Il2*$^{-/-}$ CD4$^+$ T cells (Fig. 1B). There was a trend of an increased fraction of both IFN-γ–producing (Supplemental Fig. 3) and TNF-α–producing (Supplemental Fig. 3) Th cells in the gut mucosa that was consistent with more *Il2*$^{-/-}$ and *Il2*$^{-/-}$*Il21r*$^{-/-}$ mice with TNF-α detected in the serum compared with *Il21r*$^{-/-}$ and WT mice (Fig. 6A). However, there was no significant difference between the fractions or numbers of IFN-γ– and TNF-α–producing CD4$^+$ T cells in *Il2*$^{-/-}$*Il21r*$^{-/-}$ and *Il2*$^{-/-}$ mice (Supplemental Fig. 3). Additionally, IL-21 and other STAT3 signaling cytokines can drive IL-10 production in vitro, which could ameliorate disease owing to its immunosuppressive properties (30). Despite the observed increased IL-10 gene expression in *Il2*$^{-/-}$ CD4$^+$ T cells relative to WT (Fig. 1B), the absence of IL-21/IL-21R signaling resulted in a further increase in the number of mice with circulating IL-10 and an increased fraction of IL-10–producing cells CD4$^+$ T cells (Supplemental Fig. 3).

In contrast to Th1 cells, the loss of IL-21/IL-21R signaling in *Il2*$^{-/-}$ mice reduced the percentage of IL-17A–producing Th17 cells in the lamina propria (Fig. 6C), colon epithelium (IELs) (Fig. 6D), and MLNs (Fig. 6E) to approximate that observed in *Il21r*$^{-/-}$ and WT littermates. This role for IL-21 was particularly important in gut-associated lymphoid tissue, as both the percentages (Fig. 6) and absolute numbers (Supplemental Fig. 3) were increased in the gastrointestinal tract and gastrointestinal tract–associated lymphoid tissue, but no significant difference was observed between *Il2*$^{-/-}$ and *Il2*$^{-/-}$*Il21r*$^{-/-}$ Th17 cells in the spleen (data not shown). Thus, despite the redundant role reported for IL-21/IL-21R signaling in Th17 cell generation (31), these findings support a critical role for IL-21 in Th17 cell differentiation/survival during chronic inflammation and autoimmunity.

To further investigate the high amounts of IL-22 detected in sera of *Il2*$^{-/-}$*Il21r*$^{-/-}$ mice, we detected IL-22 producing cells by intracellular immunostaining in the spleen, MLNs, Peyer's patches, IELs, and LPLs of *Il2*$^{-/-}$ and *Il2*$^{-/-}$*Il21r*$^{-/-}$ mice as well as WT and *Il21r*$^{-/-}$ mice. In accordance with previous studies (32, 33), many of the IL-22–producing cells purified from both the lamina propria and epithelial mucosa lacked expression of CD3. However, IL-22–producing cells were detected in both the αβ T cell (Fig. 6F, 6G) and NKT cell (Fig. 7H, 7I) populations. Both the *Il2*$^{-/-}$ and

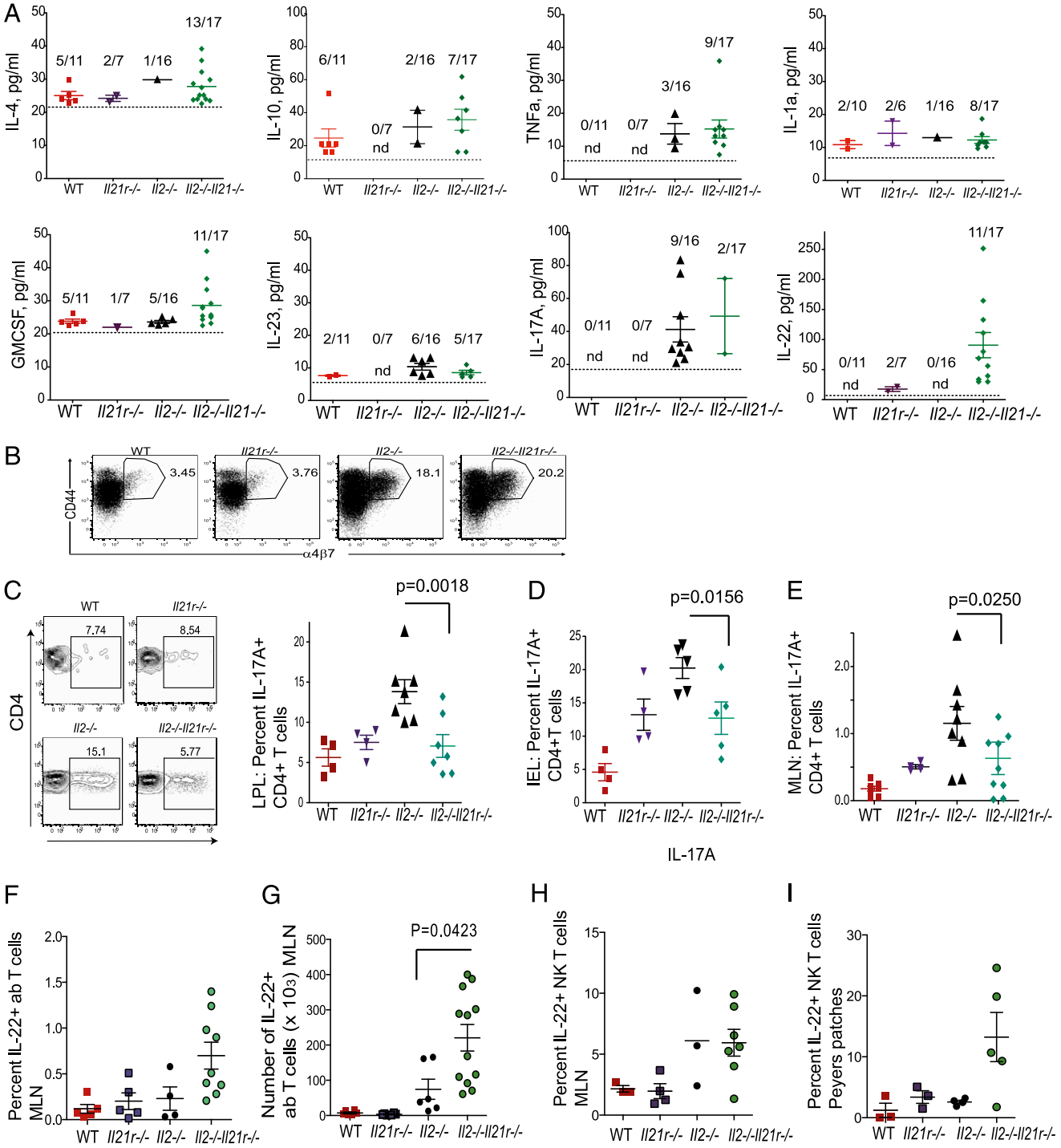

FIGURE 6. IL-21 shapes the serum cytokine profile in and Th cell differentiation in *Il2*$^{-/-}$ mice. (**A**) Cytokine bead array using a flow cytometry assay for serum cytokine levels. Data are shown as individual values for IL-4, IL-10, TNF-α, IL-1α, GM-CSF, IL-23, IL-17A, and IL-22 in pg/ml and means ± SEM detected in serum samples from mice indicated. Values were derived from individual cytokine standard curves. Mice vary in age between 6 and 24 wk, but only 6–18 wk in *Il2*$^{-/-}$ mice due to increased mortality. The *p* values were calculated using one-way ANOVA. (**B**) Representative flow cytometry dot plots of CD3^{+}CD4^{+} T cells showing activated mucosal homing CD44$^{hi}\alpha_4\beta_7{}^{+}$ subset. (**C**) Representative flow cytometry images of CD3^{+}CD4^{+} T cells from the MLNs stimulated with PMA and ionomycin for 4 h. Quantitation is shown of intracellular IL-17A staining of cells isolated from (c) LPLs, (**D**) the epithelium of the colon, and (**E**) mesenteric lymph node preparations. Quantitation of the (**F**) percentage and (**G**) absolute number of IL-22–producing αβ T cells in the MLNs and the percentage of NKT cells in the (**H**) MLNs and (**I**) Peyer's patches (PP) showing percentages from individual mice measured by intracellular immunostaining and FACS. All samples are representative of at least three experiments on mice between 8 and 12 wk of age.

Il2$^{-/-}$*21r*$^{-/-}$ strains had increased percentages and/or numbers of IL-22–producing cells relative to WT littermates (Fig. 7). Additionally, there was a trend of increased IL-22–producing αβ T cells and NKT cells in *Il2*$^{-/-}$ mice in the absence of IL-21/IL-21R signaling, which reached significance for IL-22^{+} αβ T cell numbers in the MLNs of *Il2*$^{-/-}$*Il21r*$^{-/-}$ mice (Fig. 7G). Taken together, these findings indicate that whereas IL-22^{+} cells may increase in the absence of IL-21/IL-21R signaling, the increased amount of IL-22 on the serum of *Il2*$^{-/-}$*Il21r*$^{-/-}$ mice possibly reflected deceased utilization of IL-22.

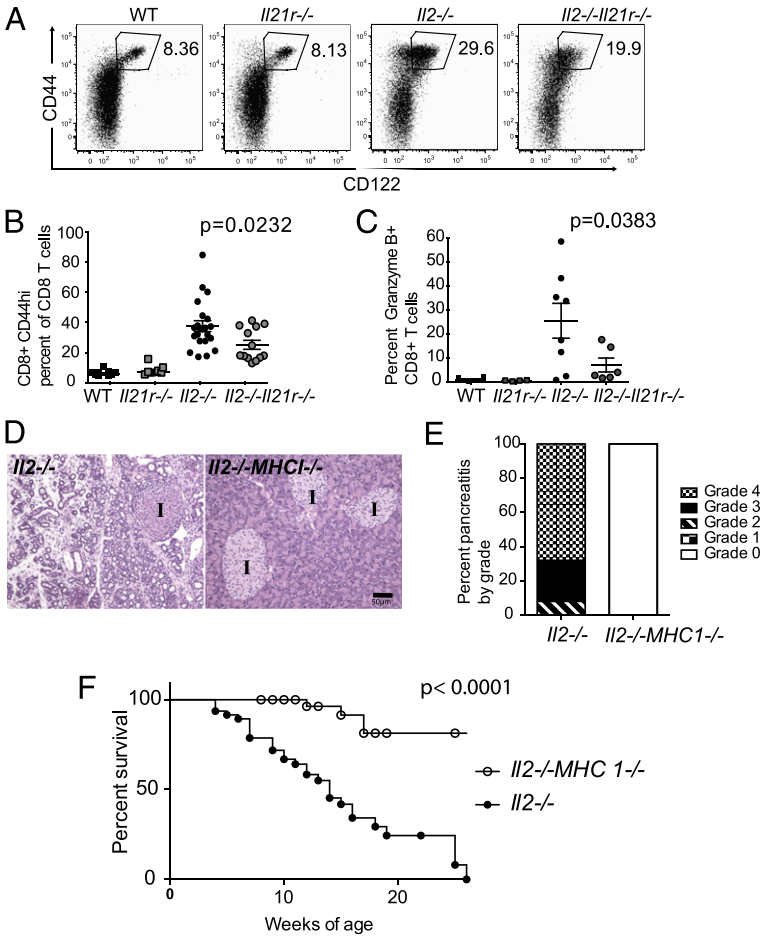

FIGURE 7. IL-21. (**A**) Representative dot plots showing expansion of the $CD122^{+}CD44^{hi}$ population in the absence of IL-2, gated on $CD3^{+}CD8^{+}$ T cells from the spleen. Quantification of (**B**) $CD3^{+}CD8^{+}CD44^{hi}$ T cells and (**C**) $CD3^{+}CD8^{+}CD44^{hi}$granzyme B^{+} analyzed by flow cytometry in genotypes shown between 8 and 12 wk of age. Data are pooled from five separate experiments and are represented as values from individual mice ± SEM. The *p* values were calculated using one-way ANOVA and a Bonferroni posttest compared with WT values. (**D**) Representative H&E-stained histological sections of pancreata from $Il2^{-/-}$ and $Il2^{-/-}MHC^{-/-}$ mice (original magnification ×20). (**E**) Pancreatitis grade from H&E-stained histological sections of pancreata from $Il2^{-/-}$ and $Il2^{-/-}MHC^{-/-}$ mice. At least 10 sections were assessed throughout the pancreas per mouse, where n = 12 for $Il2^{-/-}$ and n = 5 for $Il2^{-/-}MHC^{-/-}$ strains. (**F**) Percentage survival of $Il2^{-/-}$ (n = 31) and $Il2^{-/-}MHC^{-/-}$ mice (n = 24) was measured using euthanasia as an endpoint when mice lost 20% of their weight, or when severe morbidity was observed. The χ^2 log-rank test was used to compare survival curves.

$CD8^{+}$ T cells are important for the development of pancreatitis in $Il2^{-/-}$ mice

Similarly, $CD8^{+}$ T cells with a memory phenotype ($CD44^{hi}$, $CD122^{hi}$) were observed at increased percentages and frequencies in both $Il2^{-/-}$ and $Il2^{-/-}Il21r^{-/-}$ mice (Fig. 7). It was of interest to observe that the absence of IL-21/IL-21R signaling resulted in reduced numbers of memory phenotype $CD8^{+}$ T cells in the MLN (Fig. 7A, 7B). The fraction of $CD8^{+}CD44^{hi}$ cells that contained granzyme B was increased in $Il2^{-/-}$ mice relative to WT mice (Fig. 7C), as well as in $CD4^{+}$ T cells at an mRNA level (Fig. 1B). In the absence of IL-21/IL-21R signaling, the fraction of $CD8^{+}$ $CD44^{hi}$ cells that contained granzyme B was significantly reduced (Fig. 7C). Taken together, these findings indicate that IL-21 was acting to increase the fraction of memory phenotype and effector cells within the $CD8^{+}$ T cell population. We therefore determined the contribution of $CD8^{+}$ T cells to the chronic inflammation and pathology observed in $Il2^{-/-}$ mice. $Il2^{-/-}$ mice were backcrossed onto MHC class $I^{-/-}$ mice to generate $CD8^{+}$ T cell–deficient $Il2^{-/-}MHCI^{-/-}$ mice. Histological analyses of the pancreata from $Il2^{-/-}MHCI^{-/-}$ mice compared with pancreata from $Il2^{-/-}$ mice demonstrated that $CD8^{+}$ T cells crucially contributed to the pathology in the exocrine pancreas of $Il2^{-/-}$ mice (Fig. 7D), with a markedly reduced grade of pancreatitis observed in the absence of MHC class I expression (Fig. 7E). Accordingly, $Il2^{-/-}MHCI^{-/-}$ mice exhibited decreased morbidity and mortality (Fig. 7F), confirming that pancreatitis was a major factor in the reduced survival of $Il2^{-/-}$ mice.

Discussion

The $Il2^{-/-}$ mouse develops a fatal multiorgan inflammatory disease that is thought to arise from a deficiency in Tregs that are dependent on IL-2 for their growth and survival. This study tested the role of IL-21 in chronic inflammation in this robust model and demonstrates that IL-21 acts to accelerate the disease process, contributing to the high morbidity and mortality observed in $Il2^{-/-}$ mice, suggesting that an important role for Tregs is to regulate IL-21– and IL-21–producing Th cells. It was interesting to observe that despite the improved health of the $Il2^{-/-}$ $Il21r^{-/-}$ mice, the loss of IL-21/IL-21R signaling did not alter the deficiency in $Foxp3^{+}$ Tregs or the associated failure to regulate the size of the T cell compartment in secondary lymphoid organs.

$CD4^{+}$ T cells from $Il2^{-/-}$ mice expressed higher levels of IL-21 and harbored more IL-21–producing T cells than did their WT littermates. $Il2^{-/-}$ mice on a C57BL/6 background carry the linked IL-21 gene from 129 mice, and it is possible that the high expressing 129 IL-21 allele contributed to increased levels of IL-21 in $Il2^{-/-}$ mice (14). However, because an increase in IL-21 production has also been observed in $CD25^{-/-}$ mice (34), this finding may reflect the failure to regulate IL-21–producing Th cells. The expanded lymphoid compartments in both $Il2^{-/-}$ and $Il2^{-/-}Il21r^{-/-}$ mice contained IL-21 producing Th cells that coexpressed the mucosal homing integrin $\alpha_4\beta_7$. This finding was consistent with priming of the $CD4^{+}$ T cell population occurring in the gastrointestinal mucosa. The mild histological evidence of colitis but severe pancreatitis observed in our $Il2^{-/-}$ colony may reflect both strain differences and differences in commensal microorganisms between mouse colonies.

In contrast to colitis, the hemolytic anemia observed in $Il2^{-/-}$ mice is present in germ-free mice and is thus independent of microbiota (8). Previous studies demonstrate that $JH^{-/-}Il2^{-/-}$ double knockout mice do not succumb to anemia, indicating that

B cells are critical for hemolytic anemia in *Il2*$^{-/-}$ mice (25). Therefore, the reduced level of anemia in *Il2*$^{-/-}$*Il21r*$^{-/-}$ mice suggested a reduced level of pathogenic Abs. High circulating levels of cytokines such as IL-4 may drive the residual Ab response in *Il2*$^{-/-}$*Il21r*$^{-/-}$ mice and might also explain why IgE remained elevated in the absence of IL-21 (24).

Despite lower Ab concentrations detected in the serum, *Il2*$^{-/-}$ *Il21r*$^{-/-}$ B cells survived longer than their *Il2*$^{-/-}$ counterparts. It is not known why B cells disappear in *Il2*$^{-/-}$ mice, but it has been suggested to be due to overcrowding of B cell progenitors in the bone marrow by mature T cells (19). Our findings implicated IL-21 in B cell survival and differentiation. GC and plasma cells were increased in the presence of IL-21, supporting previous reports of IL-21 in plasma cell differentiation (35, 36). There were little, if any, MZ B cells in *Il2*$^{-/-}$ mice, but both *Il2*$^{-/-}$ and *Il2*$^{-/-}$*Il21r*$^{-/-}$ strains exhibited reduced MZ populations with lower levels of CD21 relative to WT mice. Because IL-21 is an important survival factor for B cells, it remains unclear why total B cell numbers are increased in the absence of IL-21/IL-21R signaling in *Il2*$^{-/-}$ mice, but may reflect the reduced overall level of inflammation in *Il2*$^{-/-}$ *Il21r*$^{-/-}$ mice. Our findings are consistent with a known B cell defect in *Il2*$^{-/-}$ mice (19), but they contrast with a previous study showing that MZ B cells are recovered to a greater extent in *CD25*$^{-/-}$*Il21r*$^{-/-}$ mice (34) than in *Il2*$^{-/-}$*Il21r*$^{-/-}$ mice. These differences may be due to the remaining influence of IL-2 on cells expressing the low-affinity receptor for IL-2 (IL-2Rγ/IL-2Rβ heterodimer) in *CD25*$^{-/-}$*Il21r*$^{-/-}$ mice.

By removing IL-21R from this system we could infer that IL-21 supported IL-17A production, particularly at mucosal sites of inflammation. A reduction in Th17 cells could contribute to decreased morbidity, as IL-17A– or IL-17F–producing cells can induce chronic intestinal inflammation when adoptively transferred into *Rag*$^{-/-}$ mice (26). The observation that IL-17A–producing Th17 cells produce IL-21, which contributes to autocrine expansion of this cell subset, offers an explanation for reduced Th17 cells in *Il2*$^{-/-}$*Il21r*$^{-/-}$ mice (27, 28). Interestingly, note that Th17 cells were not increased in *CD25*$^{-/-}$ mice (34). Because IL-2 has been shown to inhibit Th17 cell differentiation, signaling through the low-affinity IL-2 receptor may result in reduced Th17 cells in *CD25*$^{-/-}$ mice relative to *Il2*$^{-/-}$ mice.

The immunosuppressive cytokines IL-4 and IL-10 were detected more frequently in the serum of *Il2*$^{-/-}$*Il21r*$^{-/-}$ mice. Because IL-10–producing Tr1 cells have been shown to ameliorate colitis (37), it could be significant that IL-21R deficiency led to increased circulating IL-10 in *Il2*$^{-/-}$ mice. In addition to changes in cytokines that have broad systemic effects on lymphoid tissues, high amounts of the cytokine IL-22 were found in the circulation of *Il2*$^{-/-}$*Il21r*$^{-/-}$ mice. IL-22 is thought to act locally to aid remodeling and healing of nonlymphoid tissues that act as a physical barrier for immune defense (38–41). IL-22 produced by both innate and adaptive immune cells is dependent on commensal flora (42, 43) and is important for ameliorating tissue damage in models of gastrointestinal inflammation (39, 44). Both IL-21 and IL-22 interact with their receptors to activate STAT3 (41), but the subsequent survival and differentiation signals are delivered to distinct target cells. Current evidence suggests that whereas IL-21 acts on IL-21R–expressing immune cells, IL-22 supports the survival of IL-22R–expressing nonhematopoietic cells, including epithelial and pancreatic acinar cells (45). In keeping with the increased amounts of IL-22 in the sera of *Il2*$^{-/-}$*Il21r*$^{-/-}$ mice, there was a trend of increased IL-22–producing CD4$^+$ T cells and NKT cells in *Il2*$^{-/-}$*Il21r*$^{-/-}$ mice. It may be possible that the increased levels of IL-22 observed in sera reflected reduced utilization of IL-22 by *Il2*$^{-/-}$*Il21r*$^{-/-}$ mice that exhibited reduced inflammation in the pancreas that expresses high levels of the IL-22 receptor (45).

Thus, IL-21 acted to accelerate and worsen the process of chronic inflammation and autoimmune disease in *Il2*$^{-/-}$ mice. IL-21/IL-21R signaling supported the survival or differentiation of proinflammatory lymphocyte effector populations, and this was typified by the IL-21–mediated promotion of Th17 cells in the gastrointestinal tract and gut-related lymphoid tissues, as well as the relative increase in serum IL-10 and IL-22. IL-21–producing Th subsets such as Tfh cells and Th17 cells were increased in *Il2*$^{-/-}$ mice, and a major target of IL-21 was found to be CD8$^+$ T cells. The destructive pathology observed in the pancreas of *Il2*$^{-/-}$ mice was associated with an IL-21–mediated expansion of memory phenotype CD8$^+$ T cells that produced granzyme B. CD8$^+$ T cells were found to play a critical role in the pathology of *Il2*$^{-/-}$ mice as evidenced by the amelioration of pancreatitis in *Il2*$^{-/-}$ *MHCI*$^{-/-}$ mice. A role for CD8$^+$ T cells in chronic pancreatitis in *Il2*$^{-/-}$ mice has not previously been reported, but there is evidence for possible CD8$^+$ T cell involvement in human disease. Autoimmune pancreatitis has been characterized by a predominant CD8$^+$ T lymphocyte infiltration (46), and CD103$^+$CD8$^+$ T cells analogous to intestinal IELs have been observed to infiltrate the pancreas in chronic pancreatitis (47).

Taken together, these findings demonstrate that IL-21 is an important target of immune regulation and raise the possibility of therapeutic modulation of IL-21 to ameliorate chronic inflammatory disorders in the face of defective T regulatory function.

Disclosures

The authors have no financial conflicts of interest.

References

1. Fontenot, J. D., J. P. Rasmussen, M. A. Gavin, and A. Y. Rudensky. 2005. A function for interleukin 2 in Foxp3-expressing regulatory T cells. *Nat. Immunol.* 6: 1142–1151.
2. Leonard, W. J., R. Zeng, and R. Spolski. 2008. Interleukin 21: a cytokine/cytokine receptor system that has come of age. *J. Leukoc. Biol.* 84: 348–356.
3. Elsaesser, H., K. Sauer, and D. G. Brooks. 2009. IL-21 is required to control chronic viral infection. *Science* 324: 1569–1572.
4. Yi, J. S., M. Du, and A. J. Zajac. 2009. A vital role for interleukin-21 in the control of a chronic viral infection. *Science* 324: 1572–1576.
5. Attridge, K., C. J. Wang, L. Wardzinski, R. Kenefeck, J. L. Chamberlain, C. Manzotti, M. Kopf, and L. S. Walker. 2012. IL-21 inhibits T cell IL-2 production and impairs Treg homeostasis. *Blood* 119: 4656–4664.
6. Sadlack, B., H. Merz, H. Schorle, A. Schimpl, A. C. Feller, and I. Horak. 1993. Ulcerative colitis-like disease in mice with a disrupted interleukin-2 gene. *Cell* 75: 253–261.
7. Krämer, S., A. Schimpl, and T. Hünig. 1995. Immunopathology of interleukin (IL) 2-deficient mice: thymus dependence and suppression by thymus-dependent cells with an intact IL-2 gene. *J. Exp. Med.* 182: 1769–1776.
8. Contractor, N. V., H. Bassiri, T. Reya, A. Y. Park, D. C. Baumgart, M. A. Wasik, S. G. Emerson, and S. R. Carding. 1998. Lymphoid hyperplasia, autoimmunity, and compromised intestinal intraepithelial lymphocyte development in colitis-free gnotobiotic IL-2-deficient mice. *J. Immunol.* 160: 385–394.
9. Schultz, M., S. L. Tonkonogy, R. K. Sellon, C. Veltkamp, V. L. Godfrey, J. Kwon, W. B. Grenther, E. Balish, I. Horak, and R. B. Sartor. 1999. IL-2-deficient mice raised under germfree conditions develop delayed mild focal intestinal inflammation. *Am. J. Physiol.* 276: G1461–G1472.
10. Rhee, K. J., P. Sethupathi, A. Driks, D. K. Lanning, and K. L. Knight. 2004. Role of commensal bacteria in development of gut-associated lymphoid tissues and preimmune antibody repertoire. *J. Immunol.* 172: 1118–1124.
11. Hans, W., J. Schölmerich, V. Gross, and W. Falk. 2000. The role of the resident intestinal flora in acute and chronic dextran sulfate sodium-induced colitis in mice. *Eur. J. Gastroenterol. Hepatol.* 12: 267–273.
12. Waidmann, M., O. Bechtold, J. S. Frick, H. A. Lehr, S. Schubert, U. Dobrindt, J. Loeffler, E. Bohn, and I. B. Autenrieth. 2003. *Bacteroides vulgatus* protects against *Escherichia coli*-induced colitis in gnotobiotic interleukin-2-deficient mice. *Gastroenterology* 125: 162–177.
13. Simpson, S. J., E. Mizoguchi, D. Allen, A. K. Bhan, and C. Terhorst. 1995. Evidence that CD4$^+$, but not CD8$^+$ T cells are responsible for murine interleukin-2-deficient colitis. *Eur. J. Immunol.* 25: 2618–2625.
14. McGuire, H. M., A. Vogelzang, N. Hill, M. Flodström-Tullberg, J. Sprent, and C. King. 2009. Loss of parity between IL-2 and IL-21 in the NOD Idd3 locus. *Proc. Natl. Acad. Sci. USA* 106: 19438–19443.

15. Anders, S., D. J. McCarthy, Y. Chen, M. Okoniewski, G. K. Smyth, W. Huber, and M. D. Robinson. 2013. Count-based differential expression analysis of RNA sequencing data using R and Bioconductor. *Nat. Protoc.* 8: 1765–1786.
16. Trapnell, C., L. Pachter, and S. L. Salzberg. 2009. TopHat: discovering splice junctions with RNA-Seq. *Bioinformatics* 25: 1105–1111.
17. Anders, S., and W. Huber. 2010. Differential expression analysis for sequence count data. *Genome Biol.* 11: R106.
18. Kanno, H., M. Nose, J. Itoh, Y. Taniguchi, and M. Kyogoku. 1992. Spontaneous development of pancreatitis in the MRL/Mp strain of mice in autoimmune mechanism. *Clin. Exp. Immunol.* 89: 68–73.
19. Schultz, M., S. H. Clarke, L. W. Arnold, R. B. Sartor, and S. L. Tonkonogy. 2001. Disrupted B-lymphocyte development and survival in interleukin-2-deficient mice. *Immunology* 104: 127–134.
20. Vogelzang, A., H. M. McGuire, D. Yu, J. Sprent, C. R. Mackay, and C. King. 2008. A fundamental role for interleukin-21 in the generation of T follicular helper cells. *Immunity* 29: 127–137.
21. Nurieva, R. I., Y. Chung, D. Hwang, X. O. Yang, H. S. Kang, L. Ma, Y. H. Wang, S. S. Watowich, A. M. Jetten, Q. Tian, and C. Dong. 2008. Generation of T follicular helper cells is mediated by interleukin-21 but independent of T helper 1, 2, or 17 cell lineages. *Immunity* 29: 138–149.
22. Linterman, M. A., L. Beaton, D. Yu, R. R. Ramiscal, M. Srivastava, J. J. Hogan, N. K. Verma, M. J. Smyth, R. J. Rigby, and C. G. Vinuesa. 2010. IL-21 acts directly on B cells to regulate Bcl-6 expression and germinal center responses. *J. Exp. Med.* 207: 353–363.
23. Suzuki, K., and S. Fagarasan. 2009. Diverse regulatory pathways for IgA synthesis in the gut. *Mucosal Immunol.* 2: 468–471.
24. Geha, R. S., H. H. Jabara, and S. R. Brodeur. 2003. The regulation of immunoglobulin E class-switch recombination. *Nat. Rev. Immunol.* 3: 721–732.
25. Ma, A., M. Datta, E. Margosian, J. Chen, and I. Horak. 1995. T cells, but not B cells, are required for bowel inflammation in interleukin 2-deficient mice. *J. Exp. Med.* 182: 1567–1572.
26. Leppkes, M., C. Becker, I. I. Ivanov, S. Hirth, S. Wirtz, C. Neufert, S. Pouly, A. J. Murphy, D. M. Valenzuela, G. D. Yancopoulos, et al. 2009. RORγ-expressing Th17 cells induce murine chronic intestinal inflammation via redundant effects of IL-17A and IL-17F. *Gastroenterology* 136: 257–267.
27. Korn, T., E. Bettelli, W. Gao, A. Awasthi, A. Jager, T. B. Strom, M. Oukka, and V. K. Kuchroo. 2007. IL-21 initiates an alternative pathway to induce proinflammatory T_H17 cells. *Nature* 448: 484–487.
28. Wei, L., A. Laurence, K. M. Elias, and J. J. O'Shea. 2007. IL-21 is produced by TH17 cells and drives IL-17 production in a STAT3-dependent manner. *J. Biol. Chem.* 282: 34605–34610.
29. Hsu, W., W. Zhang, K. Tsuneyama, Y. Moritoki, W. M. Ridgway, A. A. Ansari, R. L. Coppel, Z. X. Lian, I. Mackay, and M. E. Gershwin. 2009. Differential mechanisms in the pathogenesis of autoimmune cholangitis versus inflammatory bowel disease in interleukin-2Rα$^{-/-}$ mice. *Hepatology* 49: 133–140.
30. Stumhofer, J. S., J. S. Silver, A. Laurence, P. M. Porrett, T. H. Harris, L. A. Turka, M. Ernst, C. J. Saris, J. J. O'Shea, and C. A. Hunter. 2007. Interleukins 27 and 6 induce STAT3-mediated T cell production of interleukin 10. *Nat. Immunol.* 8: 1363–1371.
31. Sonderegger, I., J. Kisielow, R. Meier, C. King, and M. Kopf. 2008. IL-21 and IL-21R are not required for development of Th17 cells and autoimmunity in vivo. *Eur. J. Immunol.* 38: 1833–1838.
32. Satoh-Takayama, N., S. Lesjean-Pottier, P. Vieira, S. Sawa, G. Eberl, C. A. Vosshenrich, and J. P. Di Santo. 2010. IL-7 and IL-15 independently program the differentiation of intestinal CD3$^-$NKp46$^+$ cell subsets from Id2-dependent precursors. *J. Exp. Med.* 207: 273–280.
33. Colonna, M. 2009. Interleukin-22-producing natural killer cells and lymphoid tissue inducer-like cells in mucosal immunity. *Immunity* 31: 15–23.
34. Tortola, L., K. Yadava, M. F. Bachmann, C. Müller, J. Kisielow, and M. Kopf. 2010. IL-21 induces death of marginal zone B cells during chronic inflammation. *Blood* 116: 5200–5207.
35. Ozaki, K., R. Spolski, R. Ettinger, H. P. Kim, G. Wang, C. F. Qi, P. Hwu, D. J. Shaffer, S. Akilesh, D. C. Roopenian, et al. 2004. Regulation of B cell differentiation and plasma cell generation by IL-21, a novel inducer of Blimp-1 and Bcl-6. *J. Immunol.* 173: 5361–5371.
36. Ettinger, R., G. P. Sims, A. M. Fairhurst, R. Robbins, Y. S. da Silva, R. Spolski, W. J. Leonard, and P. E. Lipsky. 2005. IL-21 induces differentiation of human naive and memory B cells into antibody-secreting plasma cells. *J. Immunol.* 175: 7867–7879.
37. Groux, H., A. O'Garra, M. Bigler, M. Rouleau, S. Antonenko, J. E. de Vries, and M. G. Roncarolo. 1997. A CD4$^+$ T-cell subset inhibits antigen-specific T-cell responses and prevents colitis. *Nature* 389: 737–742.
38. Zenewicz, L. A., G. D. Yancopoulos, D. M. Valenzuela, A. J. Murphy, M. Karow, and R. A. Flavell. 2007. Interleukin-22 but not interleukin-17 provides protection to hepatocytes during acute liver inflammation. *Immunity* 27: 647–659.
39. Zenewicz, L. A., G. D. Yancopoulos, D. M. Valenzuela, A. J. Murphy, S. Stevens, and R. A. Flavell. 2008. Innate and adaptive interleukin-22 protects mice from inflammatory bowel disease. *Immunity* 29: 947–957.
40. Eyerich, S., K. Eyerich, D. Pennino, T. Carbone, F. Nasorri, S. Pallotta, F. Cianfarani, T. Odorisio, C. Traidl-Hoffmann, H. Behrendt, et al. 2009. Th22 cells represent a distinct human T cell subset involved in epidermal immunity and remodeling. *J. Clin. Invest.* 119: 3573–3585.
41. Pickert, G., C. Neufert, M. Leppkes, Y. Zheng, N. Wittkopf, M. Warntjen, H. A. Lehr, S. Hirth, B. Weigmann, S. Wirtz, et al. 2009. STAT3 links IL-22 signaling in intestinal epithelial cells to mucosal wound healing. *J. Exp. Med.* 206: 1465–1472.
42. Satoh-Takayama, N., C. A. Vosshenrich, S. Lesjean-Pottier, S. Sawa, M. Lochner, F. Rattis, J. J. Mention, K. Thiam, N. Cerf-Bensussan, O. Mandelboim, et al. 2008. Microbial flora drives interleukin 22 production in intestinal NKp46$^+$ cells that provide innate mucosal immune defense. *Immunity* 29: 958–970.
43. Sanos, S. L., V. L. Bui, A. Mortha, K. Oberle, C. Heners, C. Johner, and A. Diefenbach. 2009. RORγt and commensal microflora are required for the differentiation of mucosal interleukin 22-producing NKp46$^+$ cells. *Nat. Immunol.* 10: 83–91.
44. Marks, B. R., H. N. Nowyhed, J. Y. Choi, A. C. Poholek, J. M. Odegard, R. A. Flavell, and J. Craft. 2009. Thymic self-reactivity selects natural interleukin 17-producing T cells that can regulate peripheral inflammation. *Nat. Immunol.* 10: 1125–1132.
45. Aggarwal, S., M. H. Xie, M. Maruoka, J. Foster, and A. L. Gurney. 2001. Acinar cells of the pancreas are a target of interleukin-22. *J. Interferon Cytokine Res.* 21: 1047–1053.
46. Li, S. Y., X. Y. Huang, Y. T. Chen, Y. Liu, and S. Zhao. 2011. Autoimmune pancreatitis characterized by predominant CD8$^+$ T lymphocyte infiltration. *World J. Gastroenterol.* 17: 4635–4639.
47. Ebert, M. P., K. Ademmer, F. Müller-Ostermeyer, H. Friess, M. W. Büchler, W. Schubert, and P. Malfertheiner. 1998. CD8$^+$CD103$^+$ T cells analogous to intestinal intraepithelial lymphocytes infiltrate the pancreas in chronic pancreatitis. *Am. J. Gastroenterol.* 93: 2141–2147.